Modeling deep soil properties on California grassland hillslopes using LiDAR digital elevation models

Yang Lin[1*‡], Samuel E. Prentice III[2], Tom Tran[1], Nina L. Bingham[1], Jennifer Y. King[1], and Oliver A. Chadwick[1]

[1] Department of Geography, University of California, Santa Barbara, CA 93106

[2] US Department of Agriculture - Forest Service, Payette National Forest, New Meadows, ID 83654

[*] Corresponding author Yang Lin: ylin@geog.ucsb.edu

‡ Present address: Department of Environmental Science, Policy, and Management, University of California, Berkeley, CA 94720

Journal: *Geoderma Regional*

Abstract

Topography strongly regulates soil formation at the hillslope scale through its effects on sediment redistribution and biological activities. Spatially explicit land surface parameters (LSPs) such as slope and curvature hold potential for modeling the resulting soil carbon (C) and nitrogen (N) distributions, but their representation of deep soil profiles remains largely unexplored. In this study we examine relationships between deep soil profile C and N stocks and LSPs derived from a fine-resolution digital elevation model (DEM) on prototypical rolling hillslope catenas. Consistent with other studies we found that soil thickness was the primary controller of soil organic C and N stocks and was best predicted by mean curvature. Specifically, subsoil thickness, instead of A horizon thickness, explained variability of soil C and N on hillslopes. In addition, our results suggest that, along ridge to toeslope catenas, the processes mediating soil C and N distribution varied from convex to concave positions. Convex ridge positions appeared to favor processes that enrich soil profiles with high C and N concentrations despite their drier position, while concave hollow and toeslope positions favored cumulic processes, despite their conceptually moister conditions in which enrichment processes would be favored. Our data also point to slope aspect as a weak but potentially geomorphically important covariate in modeling soil thickness and C and N stocks using LSPs. Overall, LSPs of curvature and aspect explained 51% of the variability in soil thickness, while curvature and aspect explained 50% of the variability in soil organic C stocks. Our results suggest that diffusive sediment transportation likely exerts a first-order control on soil thickness and soil organic C and N stocks in many arid landscapes. Our data also highlight the importance of subsoil in mapping soil C and N stocks and other soil

properties. Quantitative modeling of soil C and N as in our study supports examination of additional ecosystem properties at fine spatial scales.

Keywords

Mollisols, Kastanozems, deep soil carbon, geomorphology, digital soil mapping, remote sensing, DEM, pedogenic carbonate, compound topographic index, topographic wetness index

1. Introduction

Among the five soil forming factors (Jenny, 1941), continental-scale climate imposes the first-order control on soil organic and inorganic carbon accumulation (Eswaran et al., 1993; Jenny and Leonard, 1934). Catchment-scale soil carbon (C) patterns, on the other hand, are controlled by topographically sensitive processes of detachment, transportation, and deposition of soil mass driven by variations in water movement (Chamran et al., 2002; Silver et al., 2010; Yoo et al., 2006). Local relief also mediates biological C cycling (Berhe et al., 2012; Chamran et al., 2002) and consequently soil C accumulation (Hancock et al., 2010). Given that topography correlates with spatial variations in both soil mass and water redistribution, hillslopes have become a representative scale for estimating and mapping soil C stocks (Dlugoß et al., 2010; Garten and Ashwood, 2002; Hoffmann et al., 2014). Hillslopes are repeatable units in landscapes that can be upscaled or downscaled to model the spatial distribution of ecosystem and hydrological properties (e.g. soil C) (Band et al., 1993; Haas et al., 2013; Niu et al., 2014).

Characterizing soil C stocks conventionally requires field campaigns guided by soil-landscape concept models, with sparse observations qualitatively extrapolated to similar landforms and topographic positions (Hudson, 1990). Increasingly, the proliferation of digital elevation models (DEMs) enables spatially explicit prediction of static soil properties from continuous land surface parameters (LSPs) such as slope, aspect, curvature, and specific catchment area (Gessler et al., 2000; McBratney et al., 2011; Moore et al., 1993). The tight coupling of topography and soil development is sufficiently strong that LSPs are a core component of most spatially explicit predictive soil models (McBratney et al., 2003).

Among LSPs used for modeling soil C stocks, curvature is an effective representation of *in situ* hillslope processes. In contrast to slope gradient, which describes the angle of a surface to the horizontal and represents the rate of soil transport and the residence time of soil particles (Yoo et al., 2007), curvature is the rate of change in slope gradient and therefore captures patterns of convergence and divergence of soil mass flux across hillslopes. Thus, as an indicator of soil mass redistribution and soil organic C accumulation in downslope positions, curvature therefore is a preferable LSP to slope gradient (Braun et al., 2001; Van Oost et al., 2009; Yoo and Mudd, 2008). For instance using curvature, Yoo et al. (2006) found that concave positions had higher concentrations of soil C than convex positions in two soil mantled hillslopes in Northern California.

Aspect is a second LSP that provides spatial characterization of how features such as varying solar insolation and water balance can influence soil depth and C storage on hillslopes. Water budget and biological activity differ between north- and south-facing slopes; thus aspect exerts a strong impact on the landscape patterns of soil C stocks (Garcia-Pausas et al., 2007; Rezaei and Gilkes, 2005; Thompson and Kolka, 2005). For example, Rezaei and Gilkes (2005) found that surface soil organic C concentration was approximately 40% higher on the north-facing than on the south-facing slopes in an Iranian semi-arid grassland.

Although examples of spatially explicit C maps are plentiful (e.g., Dlugoß et al., 2010; Garcia-Pausas et al., 2007; Hancock et al., 2013), most focus on surface soils (10-30 cm) (Minasny et al., 2013), reflecting dataset and sampling limitations and a historical emphasis on plant-soil interactions in the upper rooting zone. This trend implicitly discounts an acknowledged large pool of deep subsoil carbon and the mechanisms that dictate this pool. Global estimates have shown that, compared to the top meter of soil, C stocks in the second and third meters increase net soil C stocks by 33 and 23%, respectively (Jobbágy and Jackson, 2000). In particular, the fractional contributions of subsoil C in arid and semi-arid ecosystems were higher than in more mesic ecosystems (Jobbágy and Jackson, 2000). A regional study found that soil thickness could reasonably predict soil C stocks in California grasslands, highlighting the important contribution of subsoil C stocks (Silver et al., 2010). Chamran et al. (2002) and Fierer et al. (2003) have offered insights into the hydrologic and biological factors that drive full profile patterns in deep soils. These examples suggest that we can improve estimates of landscape-scale C stocks, if we can use LSPs such as curvature and aspect to improve prediction of soil thickness and therefore deep C storage. However, few studies have characterized the relationships among LSPs, soil thickness and full profile C stocks on hillslopes in California grasslands.

Here we explore the relationships among soil depth, carbon stocks, and topography in a semi-arid rolling hillslope mantled with thick, bioturbated soils. Broadly, grasslands cover about 50% of California and are particularly common in the central and southern part of the state where they are sustained by a human induced fire regime and a strongly seasonal Mediterranean climate that supports cool-season C fixation and leaching prior to soil drying during the period from April to June. Water balance varies systematically across the landscape (Chamran et al., 2002; Gessler et al., 2000), so concave soil positions may show deep C accumulation whereas pedogenic carbonates may accumulate in B horizons in convex positions. Locally, soil creep and rodent burrowing drive diffusive sediment transport leading to markedly smooth hillslopes (Gabet, 2000; Gabet et al., 2005). Biological activities also vary significantly across these landscapes (e.g. north- vs. south-facing slopes), as oak trees are found predominantly on the north-facing slope.

Our research goals are: 1) to identify an appropriate spatial resolution for modeling soil properties at the hillslope scales represented by the California landscapes under consideration; 2) to explore the relationship between soil thickness and soil C and N pools; 3) to model soil C and N pools using land surface parameters (LSPs; e.g. curvature and aspect); and 4) to examine the contribution of soil depth and pedogenic carbonates to full-profile soil C and N stocks. We hypothesized that concave locations would favor accumulation of soil mass, C, and N over convex locations; that north-facing hillslope positions would have higher soil C and N storage than south-facing slopes; and that curvature and aspect would be more effective in predicting soil C and N pools than other LSPs, such as slope (Van Oost et al., 2009; Yoo and Mudd, 2008).

2. Materials and Methods

2.1 Study Site

This study was conducted at Sedgwick Reserve, one of the University of California's Natural Reserve System sites, located in the San Rafael Mountains within the California Coast Range, 45 km north of the city of Santa Barbara (43°42'N, 120°2'W; Fig. 1). Elevations at the Reserve range from 290 to 790 m, mean annual temperature is 16.8 °C, and mean annual precipitation is 380 mm. The Reserve is characterized by a Mediterranean climate with hot, dry summers and cool, wet winters with strong interannual variations (max = 923 mm, min = 167 mm, coefficient of variation = 0.48). Overland flow on hillslopes is rare owing to extensive subsurface flow paths from large populations of fossorial mammals (Chamran et al., 2002; Davis et al., 2011). The study site features an oak savannah community dominated by Mediterranean grasses *Bromus diandrus*, *B. hordaceous*, and *Avena fatua,* with scattered coast live oaks (*Quercus agrifolia*), valley oaks (*Quercus lobata*), and blue oaks (*Quercus douglasii).* Oak tree density of the site is approximately 1.2 stems/ha with height varying from 12 to 25 m (Sork et al., 2002).

Sampled hillslopes constitute a dissected fanglomerate with smooth slopes converging to hollows with no incised channels. Overlying soils have formed from weathering of the Paso Robles formation, a Plio-Pleistocene, weakly consolidated subaerial alluvial deposit composed of variable amounts of marine shale and mélange siltstones, chert, and serpentine (Dibblee, 1966). Effective depth of wetting is evidenced by small amounts of finely disseminated pedogenic carbonate and carbonate masses precipitated in subsoil horizons. Hillslope soils are mapped as Xerorthents by the USDA Soil Conservation Service (1972). Most soils on the hillslopes we sampled are classified as Haploxerolls based on thickness, color, and minimum 0.6% carbon content in the epipedon (Table 1).

2.2 Soil sampling and laboratory analyses

We sampled soils on north- and south-facing hillslopes flanking a broad aggradational valley. The hillslopes are approximately 150 m wide by 200 m long and include both convex and concave slope elements but no incised stream channels (Fig. 1). Two catenas were transected across ridge, shoulder, backslope, and toeslope positions, capturing a representative range of convexity, concavity, and aspect. Sixteen locations were sampled in total. Soils were excavated to bedrock, described using standard field procedures (Schoeneberger et al., 2002), and channel sampled by horizon to achieve equal representation from upper to lower boundaries. The Saran clod method (Soil Survey Division Stuff, 1993) was used to measure bulk densities, and values were corrected for linear extensibility at 33% smectitic clay content based on mean particle size distribution values from previous work in the area (Gessler et al., 2000). At locations requiring hand augering to reach bedrock, bulk density was estimated by correlating with hand samples from similar horizons in this study. Soil cracks were observed and recorded when present.

Field samples were oven-dried at 105 °C, weighed, and sieved to <2 mm for elemental analysis. Rock fragment concentrations were determined by the ratio between the remaining mass of soil on the 2-mm sieve (rock) and the total soil mass. Total C and N concentrations were measured on the <2-mm fraction using an elemental analyzer (Fisons NA1500). Soil inorganic C concentration was obtained by acidifying a subsample in a sealed glass jar with 5 ml of 2N H_2SO_4 with 5% $FeSO_4$ (Loeppert and Suarez, 1996) and measuring the change in headspace CO_2 concentrations with an infrared gas analyzer (IRGA, LI-COR 6520). Calcium carbonate (grade: certified ACS) was used to build a standard curve for calibrating inorganic C measurements. This method has an accuracy of ±3% and can detect soil inorganic C concentrations ranging from 0.005% to 5%. Soil organic C concentration (% OC) was calculated by subtracting inorganic C concentration (%IC) from total C concentration. All analyses were run in duplicate, and their averages were used in the following analyses.

To determine net soil C and N stocks in soil profiles, elemental concentrations were multiplied by the bulk density of their respective parent horizons, then by respective horizon thicknesses to arrive at horizon-based mass storage at each sample location. Soil C and N stocks were also adjusted for rock fragment concentrations. Free carbonate depth was determined in the field from intact profile faces using 1M HCl based on strong effervescence (Soil Survey Division Stuff, 1993).

2.3 Terrain analyses

Land surface parameters of slope aspect (A), slope gradient (β), mean curvature (Cs), specific catchment area (As), and compound topographic index (CTI) were derived from a gridded 1-m DEM of the study area acquired using a terrestrial LiDAR scanner (RIEGL, LMS-Z420i) (Fisher et al., 2008). Mean curvature was calculated following Passalacqua et al. (2010) in which positive Cs indicates concave-convergent surfaces and negative Cs indicates convex-divergent surfaces:

$$Cs = \nabla \cdot (\nabla h / |\nabla h|)$$

in which *h* is the elevation. Slope gradient and specific catchment area were calculated using TopoToolbox terrain functions in MATLAB (Schwanghart and Kuhn, 2010). Compound topographic index (CTI; i.e., steady-state wetness index), commonly used to quantify the effects of catchment position on hydrologic drainage intensity (Gessler et al., 2000; Moore et al., 1993), was calculated in MATLAB as

$$CTI = \ln(As/\tan\beta) .$$

To identify the most statistically robust spatial resolution for predicting soil properties in our study area, the DEM was filtered (i.e., smoothed) in one-meter increments from 2 m to 45 m, and LSPs were generated directly from DEMs at each scale increment. Many filtering kernels exist, the most common being mean, median, and Gaussian. A median kernel was chosen for filtering because of its relative effectiveness in removing “salt-and-pepper” noise (Arce, 2005). Correlation coefficients between LSPs and selected soil profile properties were then calculated for each spatial resolution between 2 and 45 m in order to evaluate how spatial resolutions affect the predictive power of LSPs. Soil thickness, depth of A horizon, and free carbonate depth were chosen as proxies for scale- and depth-dependent pedogeomorphic processes operating across our hillslope catenas.

Preliminary results indicated differences in soil properties between north- and south-facing slopes, but slope aspect in degrees (0-359) did not capture these differences. We therefore simplified aspect into a binary variable based on whether the soil profile was located on the north- or the south-facing slope (Fig. 1).

2.4 Statistical analyses

Pearson correlation was applied to examine relationships among soil properties and LSPs. Differences in soil properties between the north- and south-facing slopes were compared using Student’s t-tests. During the t-test, the Welch-Satterthwaite method was used to adjust degrees of freedom if equality of variances could not be assumed according to the Levene’s test. Significance levels of correlations and t-tests were set at the $\alpha = 0.05$ level. Multiple linear regressions were used to build empirical models that predicted soil C and N stocks with LSPs. The LSPs were only included in the model if they increased the F-value at the $\alpha = 0.05$ level (forward linear regression). All statistical analyses were conducted in SPSS v20 (IBM Inc.).

3. Results

Site data and soil characteristics for full soil profiles and for A horizons as a proportion of full soil profiles are compiled in Table 1. Detailed descriptions of each sampled horizon are given in Supplementary Table 1. Mean full profile thickness was 161 cm, and mean A horizon thickness was 22 cm. Averaged across all pedons, the organic carbon mass fraction was dominant (59% of mean profile C) over the inorganic carbon mass fraction (41% of mean profile C), which is characteristic of the regional semi-arid climate and infrequent profile throughflow (Chamran 2002). In profiles, A horizons (14% of mean full profile thickness) accounted for 43% of profile organic carbon storage and 15% of profile inorganic carbon storage, reflecting biologic carbon enrichment typical of surface soil.

3.1 Correlations among soil characteristics

We first explored the correlations between soil thickness and other studied soil characteristics without linking them to LSPs. On a mass basis, full profile organic C and N stocks were strongly correlated with soil thickness (Fig. 2a, b) such that larger organic C and N stocks were associated with thicker soils. Soil thickness explained 86% and 89% of the variability of soil organic C and N stocks, respectively (both $P < 0.01$). Inorganic C stocks were weakly correlated with soil thickness (Fig. 2c) due to a thick soil profile (#15) with extremely low inorganic C. This soil pit is located in a convergent hydrogeomorphic position on the valley floor margin that is wetter and presumably more heavily leached (Fig. 1). When this location is removed from the regression, prediction of inorganic C stocks from soil thickness increases substantially ($R^2 = 0.85$, $P < 0.01$). On a constituent concentration (i.e., %) basis, thicker profiles had lower organic C (%OC) and

N concentrations (%N) compared to thinner profiles (Fig. 2d, e). Soil thickness was markedly less effective in explaining %OC and %N than explaining C and N stocks, accounting for 42% and 55% of variability of %OC and %N, respectively. Soil thickness did not correlate with inorganic C concentration (%IC, Fig. 2f).

3.2 Soil-landscape modeling

In service of linking soil properties with terrain attributes, we next examined relationships between LSPs and soil characteristics. Consistent with other works (Braun et al., 2001; Yoo et al., 2006), curvature (Cs) was the most robust indicator of soil spatial variability in the study area, showing significant correlations with both soil thickness and free carbonate depth, with local maxima coinciding at a resolution of approximately 14 m (Fig. 3). Specific catchment area (As) and compound topographic index (CTI), on the other hand, only had significant correlations with soil thickness. In addition, curvature was the only LSP that significantly explained both soil C stocks and concentrations (Fig. 4, Table 2). Thus 14 m was chosen as the spatial resolution for subsequent modeling of soil-terrain relationships.

Mean curvature (Cs) explained 42% of soil thickness variability such that concave locations (Cs > 0) had thicker soils than convex locations (Cs < 0, Fig. 4a). Full profile organic C and N stocks had comparably strong relationships with curvature, consistent with our first hypothesis that organic C and N storage is low at convex locations and increases in concave locations. Interestingly, significant relationships between curvature and soil organic C and N were observed in subsoil but not in A horizons (Supplementary Fig. 1). In contrast to organic C and N stocks, profiles in convex locations had higher %OC and %N (Fig. 4g, h). Mean curvature could not adequately explain IC stocks nor %IC variability on a whole profile basis (Fig. 4f, i). However, when considering A horizon only, IC stocks and %IC were lower in concave positions than in convex positions (Supplementary Fig. 1), a finding reflected in deeper free carbonate depth at concave locations (Fig. 4c). The ratio of soil OC to N stocks (OC/N) did not depend on curvature (data not shown).

Slope aspect (A) also affected the distribution of soil properties, though these effects were weaker than what we hypothesized. Soil profiles on the north-facing slope were approximately two times thicker than on the south-facing slope (Fig. 5a, 233 vs. 117 cm, $P = 0.16$) which led to the general trend, though not statistically significant, that organic C and N stocks were higher on the north-facing slope (Fig. 5d, e). Profile A horizons on the north-facing slope were also marginally thicker than A horizons on the south-facing slope (Fig. 5b, $P = 0.11$).

As hypothesized, LSPs other than curvature and slope aspect proved less consistent in predicting soil properties (Table 2). For instance, slope gradient (β) predicted profile OC, IC, and N concentrations, but failed to adequately explain soil thickness or stocks (Table 2). Compound topographic index (CTI) had moderately strong positive relationships with OC and N stocks but, unlike curvature, did not correlate with soil thickness. Specific catchment area (As) correlations were generally weak and nonsignificant among all studied soil properties.

Combining LSPs in multivariate linear models provided reasonable predictions of all soil properties except inorganic C. Notably, three of the four strongest models employed curvature as an explanatory variable, and two of the four strongest models employed aspect. As noted previously (Fig. 4a), Cs alone explained 42% of thickness variability, and integrating Cs and A in a linear model increased this to 51% (Table 3). A model that includes Cs and A was also effective in predicting soil organic C stocks ($R^2 = 0.50$). Variability of N stocks was best predicted by CTI alone ($R^2 = 0.42$), while N concentrations were best predicted by a combination of Cs and β ($R^2 = 0.62$). As discussed earlier, β correlated well with %OC and was therefore the dominant predictor in the %OC linear model along with Cs ($R^2 = 0.56$). A model with β explained 26% of the variability of inorganic C stock, while the LSPs we explored could not predict soil %IC. Overall, these linear models could be used to produce predictive maps of soil properties (e.g. soil thickness, soil organic C stock, and %OC) in this landscape (Supplementary Fig. 2).

4. Discussion

Our results demonstrate that soil organic C and N stocks are strongly controlled by soil thickness (Fig. 2a, b), which is both logical and consistent with earlier findings from a regional study in California (Silver et al., 2010). Furthermore, our results demonstrate that reasonable predictions of soil organic C and N stocks can be achieved by modeling soil thickness at hillslope scales using curvature and aspect (Table 3). In our study, soil thickness depends on landscape curvature such that deeper soils were found on convergent hillslope components defined by concave surfaces that increase in size and frequency downslope (Figs. 1, 4a). Given the absence of surface erosion and infrequent saturated conditions of the study area (Chamran et al., 2002), this result suggests that diffusive sediment transport and aspect-mediated processes drive the spatial procession of soil organic C and N patterns from ridge to toeslope positions. The curvature gradient is further reflected in taxonomy with inorganic C-rich Calcic subgroups in convex positions grading to cumulic Calcic Pachic subgroups in concave positions (Table 1). Our result is consistent with geomorphic process models that suggest soil-creep induced thickening from convex to concave positions on similar hillslopes (Black and Montgomery, 1991; Gabet et al., 2005).

Compared to organic C and N stocks, full-profile organic C and N concentrations had more complex relationships with local relief. Although concave locations favored accumulation of soil mass, organic C, and N, they hosted soils with lower organic C and N concentrations than convex locations (Fig. 4). This discrepancy between inventory and concentration is possible when soil organic matter is partially decomposed as soil mass is undergoing diffusive transport downslope (Berhe et al., 2008; Wang et al., 2014). The pattern may also be explained by the net balance between primary production and decomposition and its variation across the landscape. Among previous studies at our site, Tan (2014) found that aboveground biomass was similar regardless of curvature, while results from Chamran et al. (2002) and Fierer et al. (2005) suggested that recent dissolved organic C would be transported to depositional locations and preferentially decomposed in the subsurface when the soil is moist. In fact, on a similar California hillslope, Berhe et al. (2012) found that C mineralization rate (~ 25 cm soil depth) was significantly higher at the depositional positions than the eroding positions. Therefore, concave locations may stay wet longer than convex locations, especially in the subsurface (Chamran et al., 2002), and therefore exhibit a net loss of C and N in this landscape.

We also found that full-profile organic C and N concentrations varied with slope gradient such that steeper slopes were depleted and shallower slopes were enriched in soil C (Table 2). Slope gradient reflects the residence time of soil particles (Yoo et al., 2007) such that soil particles reside longer within the solum on low angle slopes. High organic C concentration at these locations thus indicates that either physical transport of organic C is low, or that biological additions of organic C are greater than physical additions. Overall, our accounting of organic C stocks and concentrations reflect different processes on these hillslopes: patterns of organic C stock were determined by the curvature-driven sediment accumulation, while organic C concentration was influenced by C gain/loss processes during sediment transport (e.g., organic matter decomposition and plant productivity).

Notably, curvature-driven variations in organic C and N stocks were determined by subsoil thickness, rather than A horizon thickness (Supplementary Fig. 1). There was also a relatively homogeneous distribution of surface horizon C concentrations among hillslope positions (Supplementary Fig. 1), consistent with other Mediterranean ecosystems (Hancock et al., 2013; Yoo et al., 2006). Furthermore, subsoil contributed more to the soil organic C and N stocks than the A horizons (Table 1). These results highlight the importance of incorporating deeper soil horizons into the quantification of soil C and N stocks. They also imply that utilization of terrain attributes to predict soil C and N stocks in surface soils may lead to error in diffusive hillslope landscapes. These results support previous studies (e.g., Jobbágy and Jackson, 2000; Rumpel and Kögel-Knabner, 2010) that argue that incorporation of subsoil carbon analyses is critically important to fully characterize and model the landscape distribution of carbon.

Our results are consistent with previous studies that have found similar curvature-dependency of soil thickness in semi-arid environments in California, Australia, and Italy (Braun et al., 2001; Catani et al., 2010; Heimsath et al., 1997; Minasny and McBratney, 2006). Our site shares many key characteristics with the landscapes in the above studies: they are all low-relief, soil-mantled hillslopes that are dominated by diffusive processes. Together with other studies, our results support the idea that curvature is the dominant control of soil mass and thickness in diffusive landscapes in semi-arid environments. Soil thickness further explains a great proportion of the variations in soil organic C and N stocks (Fig. 2) likely because plant productivity and decomposition are water limited in these semi-arid environments. Landscape analysis thus has great potential to accurately model soil thickness and soil organic C and N stocks in these ecosystems.

As demonstrated, curvature is the most effective LSP for predicting a wide range of hillslope soil characteristics from soil thickness and C and N stocks to C and N concentrations (Fig. 4, Table 2). Among all LSPs, only curvature has a significant relationship with soil thickness, and no other LSPs had significant correlations with both organic C stock and its concentration. In terms of predicting soil N stock, curvature is as effective as CTI (correlation coefficient: 0.669 vs. 0.677). This result is not surprising, given that CTI describes the differences in flow and sediment accumulation across the landscape (Gessler et al., 2000). However, the slightly higher correlation coefficient between CTI and N stock explains why CTI, not curvature, is selected in the final linear regression model of the soil N stock (Table 3).

Grouping sites according to north- and south-facing aspects revealed marginal differences in thickness and mass-based indicators, but not concentration-based indicators (Fig. 5d, e). It is well known that slope aspect casts a strong influence on solar insolation, microclimate, and plant community (Burnett et al., 2008; Istanbulluoglu et al., 2008; Panizza and Panizza, 1996). Thus oak trees are only found on the north-facing slope, and aboveground productivity was higher on the north-facing than on the south-facing slope (Tan, 2014). These aspect-induced differences in plant community and productivity likely explain the thicker A horizons on the north-facing slope (Fig. 5b). The difference in the thickness of A horizon, not surprisingly, led to higher C and N stocks of the A horizon on the north-facing than on the south-facing slope (data not shown). The north-facing slope tended to have deeper soil and higher whole-profile organic C and N stocks; however, these differences were not significant (Fig. 5a, d, e). Our results thus suggest that while curvature exerts a strong first-order control on soil development, aspect-related differences in biological processes play an important secondary role. It is also likely that aspect-induced differences in biological processes have only occurred in a shorter time scale compared to the diffusion processes. Furthermore, these results imply that the aspect-driven biological differences mostly affect soil characteristics in surface horizons.

Distribution of soil inorganic C in the landscape was distinctly different from soil organic C. Unlike soil organic C, inorganic C stock was not predicted by curvature (Fig. 4f). Free carbonate depth did have a positive relationship with curvature, and carbonate started accumulating in surface horizons (free carbonate depth $\leq$ 6 cm) at the most convex locations (Fig. 4c). These results suggest that free carbonate depth was not limited by the shallow soil thickness at convex locations, but rather was indicative of landscape-controlled effective moisture and depth of wetting. Since water can easily escape the convex surfaces through short-distance overland and through-soil flow (Chamran et al., 2002), these locations were more water-limited than concave locations, thus favoring shallow infiltration depth (Fig. 4c). Mean profile inorganic C stocks were comparable to profile organic C stocks (Table 1), reflecting the semi-arid water balance of the prevailing regional climate. If, however, drought becomes more persistent and severe (Cook et al., 2015), the balance of these C pools would likely shift towards greater accumulation of inorganic C relative to organic C. Our results demonstrate that terrain analysis offers valuable insights into understanding variation in local infiltration and hence the distribution of soil inorganic C stock.

Our results suggest that for gently to moderately rolling hills in California and elsewhere, medium resolution DEMs (10 to 15 m) are suitable for modeling soil thickness and full profile organic C and N stocks (Fig. 2). At finer scales (e.g. 1 m), LSPs characterize surface roughness features (e.g., gopher mounds) that, while playing a crucial mechanistic role in shaping hillslope and affecting soil C patterns, do not meaningfully contribute to static soil property prediction (Supplementary Fig. 3). At scales coarser than 15 m, LSPs become increasingly ineffective at modeling soil properties (e.g. carbonate accumulation, Fig. 2a) as landscape variability is homogenized. Along with other studies (Kienzle, 2004; Liu, 2008), results here indicate that applying fine-resolution DEMs to digital soil mapping requires careful and thoughtful consideration of spatially coupled soil processes and properties (Supplementary Fig. 3).

5. Conclusions

Overall, our data suggest that subsoil characteristics, rather than surface soil characteristics, best describe the spatial patterns of soil C and N stocks in landscapes that are mainly shaped by diffusive sediment transport. These relationships can be adequately modeled in hillslope landscapes using LSPs, specifically curvature and aspect, which reflect processes actively mediating full profile soil thickening. Given that similar curvature-dependency of soil thickness has been commonly observed in other diffusive landscapes (Braun et al., 2001; Catani et al., 2010; Heimsath et al., 1997; Minasny and McBratney, 2006), our results support the idea that high resolution DEMs have great potential to accurately model soil thickness and soil organic C and N stocks in semi-arid ecosystems. Landscape analysis also proves valuable in understanding the spatial distribution of inorganic C in dry environments. Using a combination of detailed empirical measurements and remotely sensed terrain information, we produced quantitative models of soil C and N stocks at the hillslope scale. These models provide key insight into the processes that shape landscape patterns of soil C and N stocks. Thus our models allow the development of hypotheses about how soil C and N storage may change under changing conditions and enable examination of soil C and N stocks in similar diffusive-transport-dominated landscapes.

Acknowledgements

We thank William Barnes, Ken Marchus, Kaelyn Schwartz, Zhareen Bulalacao, Kana Yamamoto, and Keri Opalk for assisting in the field and laboratory. We thank Kate McCurdy and the University of California's Sedgwick Reserve for providing the site and logistical support. Comments from Alfred Hartemink and two anonymous reviewers improved this article. YL was supported in part by a Graduate Division Dissertation Fellowship, University of California, Santa Barbara.

References

Arce, G.R., 2005. Nonlinear Signal Processing: A statistical Approach. Wiley, New Jersey, USA.

Band, L.E., Patterson, P., Nemani, R., Running, S.W., 1993. Forest ecosystem processes at the watershed scale: incorporating hillslope hydrology. Agric. For. Meteorol. 63, 93-126.

Berhe, A.A., Harden, J.W., Torn, M.S., Harte, J., 2008. Linking soil organic matter dynamics and erosion-induced terrestrial carbon sequestration at different landform positions. J. Geophys. Res. -Biogeo. 113, 1-12.

Berhe, A.A., Harden, J.W., Torn, M.S., Kleber, M., Burton, S.D., Harte, J., 2012. Persistence of soil organic matter in eroding versus depositional landform positions. J. Geophys. Res. -Biogeo. 117.

Black, T.A., Montgomery, D.R., 1991. Sediment transport by burrowing mammals, Marin County, California. Earth Surf. Proc. Land. 16, 163-172.

Braun, J., Heimsath, A.M., Chappell, J., 2001. Sediment transport mechanisms on soil-mantled hillslopes. Geology 29, 683-686.

Burnett, B.N., Meyer, G.A., McFadden, L.D., 2008. Aspect ‐ related microclimatic influences on slope forms and processes, northeastern Arizona. J. Geophys. Res. -Earth Surf. 113, F03002.

Catani, F., Segoni, S., Falorni, G., 2010. An empirical geomorphology ‐ based approach to the spatial prediction of soil thickness at catchment scale. Water Resour. Res. 46, W05508.

Chamran, F., Gessler, P.E., Chadwick, O.A., 2002. Spatially explicit treatment of soil-water dynamics along a semiarid catena. Soil Sci. Soc. Am. J. 66, 1571-1583.

Cook, B.I., Ault, T.R., Smerdon, J.E., 2015. Unprecedented 21st century drought risk in the American Southwest and Central Plains. Sci. Adv. 1, e1400082.

Davis, F.W., Tyler, C.M., Mahall, B.E., 2011. Consumer control of oak demography in a Mediterranean-climate savanna. Ecosphere 2, art108.

Dibblee, T., 1966. Santa Ynez Mountains: Geology of the Central Santa Ynez Mountains Santa Barbara County, California. Department of Conservation, California Division of Mines and Geology.

Dlugoß, V., Fiener, P., Schneider, K., 2010. Layer-specific analysis and spatial prediction of soil organic carbon using terrain attributes and erosion modeling. Soil Sci. Soc. Am. J. 74, 922-935.

Eswaran, H., Van Den Berg, E., Reich, P., 1993. Organic carbon in soils of the world. Soil Sci. Soc. Am. J. 57, 192-194.

Fierer, N., Allen, A., Schimel, J.P., Holden, P.A., 2003. Controls on microbial CO2 production: a comparison of surface and subsurface soil horizons. Global Change Biol. 9, 1322-1332.

Fierer, N., Chadwick, O.a., Trumbore, S.E., 2005. Production of CO_2 in soil profiles of a California annual grassland. Ecosystems 8, 412-429.

Fisher, G., Bookhagen, B., Perroy, R.L., Burbank, D., 2008. Exploring channel initiation thresholds across varying resolutions of topography and DEM creation techniques. American Geophyiscal Union, Fall meeting 2008, abstract #H53B-1022.

Gabet, E.J., 2000. Gopher bioturbation: Field evidence for non-linear hillslope diffusion. Earth Surf. Proc. Land. 25, 1419-1428.

Gabet, E.J., Fierer, N., Chadwick, O.A., 2005. Prediction of sediment ‐ bound nutrient delivery from semi ‐ arid California watersheds. J. Geophys. Res. -Biogeo. 110, G02001.

Garcia-Pausas, J., Casals, P., Camarero, L., Huguet, C., Sebastia, M.-T., Thompson, R., Romanya, J., 2007. Soil organic carbon storage in mountain grasslands of the Pyrenees: effects of climate and topography. Biogeochemistry 82, 279-289.

Garten, C.T., Ashwood, T.L., 2002. Landscape level differences in soil carbon and nitrogen: implications for soil carbon sequestration. Global Biogeochem. Cycles 16, 1114.

Gessler, P.E., Chadwick, O.A., Chamran, F., Althouse, L., Holmes, K., 2000. Modeling soil–landscape and ecosystem properties using terrain attributes. Soil Sci. Soc. Am. J. 64, 2046-2056.

Haas, E., Klatt, S., Fröhlich, A., Kraft, P., Werner, C., Kiese, R., Grote, R., Breuer, L., Butterbach-Bahl, K., 2013. LandscapeDNDC: a process model for simulation of biosphere–atmosphere–hydrosphere exchange processes at site and regional scale. Landscape Ecol. 28, 615-636.

Hancock, G.R., Murphy, D., Evans, K.G., 2010. Hillslope and catchment scale soil organic carbon concentration: An assessment of the role of geomorphology and soil erosion in an undisturbed environment. Geoderma 155, 36-45.

Hancock, G.R., Murphy, D.V., Li, Y., 2013. Soil properties and environmental tracers: A DEM based assessment in an Australian Mediterranean environment. Geomorphology 183, 45-57.

Heimsath, A.M., Dietrich, W.E., Nishiizumi, K., Finkel, R.C., 1997. The soil production function and landscape equilibrium. Nature 388, 358-361.

Hoffmann, U., Hoffmann, T., Johnson, E.A., Kuhn, N.J., 2014. Assessment of variability and uncertainty of soil organic carbon in a mountainous boreal forest (Canadian Rocky Mountains, Alberta). Catena 113, 107-121.

Hudson, B.D., 1990. Concepts of soil mapping and interpretation. Soil Surv. Horiz. 31, 63-73.

Istanbulluoglu, E., Yetemen, O., Vivoni, E.R., Gutiérrez‐Jurado, H.A., Bras, R.L., 2008. Eco‐geomorphic implications of hillslope aspect: Inferences from analysis of landscape morphology in central New Mexico. Geophys. Res. Lett. 35, L14403.

Jenny, H., 1941. The factors of soil formation. McGraw-Hill, New York.

Jenny, H., Leonard, C.D., 1934. Functional relationships between soil properties and rainfall. Soil Sci. 38, 363-382.

Jobbágy, E.G., Jackson, R.B., 2000. The vertical distribution of soil organic carbon and its relation to climate and vegetation. Ecol. Appl. 10, 423-436.

Kienzle, S., 2004. The Effect of DEM Raster Resolution on First Order, Second Order and Compound Terrain Derivatives. Transactions in GIS 8, 83-111.

Liu, X., 2008. Airborne LiDAR for DEM generation: some critical issues. Prog. Phys. Geogr 32, 31-49.

Loeppert, R.H., Suarez, D.L., 1996. Carbonate and gypsum. In: D.L. Sparks (Ed.), Methods of Soil Analysis. Part 3—SSSA Book Series n.5. . ASA and SSSA, Madison, WI, USA, pp. 437-474.

McBratney, A.B., Minasny, B., MacMillan, R.A., Carré, F., 2011. Digital Soil Mapping. In: P.M. Huang, Y.C. Li, M.E. Sumner (Eds.), Handbook of Soil Sciences, Properties and Processes, Second Edition. CRC Press, New York, pp. 1-44.

McBratney, A.B., Santos, M.L.M., Minasny, B., 2003. On digital soil mapping. Geoderma 117, 3-52.

Minasny, B., McBratney, A.B., 2006. Mechanistic soil–landscape modelling as an approach to developing pedogenetic classifications. Geoderma 133, 138-149.

Minasny, B., McBratney, A.B., Malone, B.P., Wheeler, I., 2013. Digital Mapping of Soil Carbon. In: D.L. Sparks (Ed.), Advances in Agronomy. Elsevier Inc., pp. 1-47.

Moore, I.D., Gessler, P.E., Nielsen, G.A., Peterson, G.A., 1993. Soil Attribute Prediction Using Terrain Analysis. Soil Sci. Soc. Am. J. 57, 443-452.

Niu, G.Y., Pasetto, D., Scudeler, C., Paniconi, C., Putti, M., Troch, P.A., DeLong, S.B., Dontsova, K., Pangle, L., Breshears, D.D., 2014. Incipient subsurface heterogeneity and its effect on overland flow generation–insight from a modeling study of the first experiment at the Biosphere 2 Landscape Evolution Observatory. Hydrol. Earth Syst. Sci. 18, 1873-1883.

Panizza, M., Panizza, M., 1996. Environmental Geomorphology. Elsevier B.V., Amsterdam, Netherlands.

Passalacqua, P., Do Trung, T., Foufoula‐Georgiou, E., Sapiro, G., Dietrich, W.E., 2010. A geometric framework for channel network extraction from lidar: Nonlinear diffusion and geodesic paths. J. Geophys. Res. -Earth Surf. 115, F01002.

Rezaei, S.A., Gilkes, R.J., 2005. The effects of landscape attributes and plant community on soil chemical properties in rangelands. Geoderma 125, 167-176.

Rumpel, C., Kögel-Knabner, I., 2010. Deep soil organic matter—a key but poorly understood component of terrestrial C cycle. Plant Soil 338, 143-158.

Schoeneberger, P.J., Wysocki, D.A., Benham, E.C., Broderson, W.D. (Eds.), 2002. Field book for describing and sampling soils, Version 2.0. Natural Resources Conservation Service, National Soil Survey Center, Lincoln, NE.

Schwanghart, W., Kuhn, N.J., 2010. TopoToolbox: A set of Matlab functions for topographic analysis. Environ. Model. Software 25, 770-781.

Silver, W.L., Ryals, R., Eviner, V., 2010. Soil carbon pools in California's annual grassland ecosystems. Rangeland Ecol. Manage. 63, 128-136.

Soil Survey Division Stuff, 1993. Chapter 3. Examination and Description of Soils. Soil Conservation Service. Soil survey manual, United States Department of Agriculture Handbook 18.

Sork, V.L., Davis, F.W., Smouse, P.E., Apsit, V.J., Dyer, R.J., Fernandez-M, J.F., Kuhn, B., 2002. Pollen movement in declining populations of California Valley oak, *Quercus lobata*: where have all the fathers gone? Mol. Ecol. 11, 1657-1668.

Tan, A.J., 2014. Microscale Topographic Influence on Grassland Primary Productivity on Semiarid Hillslopes. MA Thesis, University of California, Santa Barbara.

Thompson, J., Kolka, R., 2005. Soil carbon sorage estimation in a forested watershed using quantitative soil-landscape modeling. Soil Sci. Soc. Am. J. 69, 1086-1093.

USDA Soil Conservation Service, 1972. Soil survey of northern Santa Barbara County, CA. In cooperation with Univ. of California Agric. Experiment Station. U.S. Govt. Print. Office, Washington, DC.

Van Oost, K., Cerdan, O., Quine, T.A., 2009. Accelerated sediment fluxes by water and tillage erosion on European agricultural land. Earth Surf. Proc. Land. 34, 1625-1634.

Wang, X., Cammeraat, E.L.H., Cerli, C., Kalbitz, K., 2014. Soil aggregation and the stabilization of organic carbon as affected by erosion and deposition. Soil Biol. Biochem. 72, 55-65.

Yoo, K., Amundson, R., Heimsath, A.M., Dietrich, W.E., 2006. Spatial patterns of soil organic carbon on hillslopes: Integrating geomorphic processes and the biological C cycle. Geoderma 130, 47-65.

Yoo, K., Amundson, R., Heimsath, A.M., Dietrich, W.E., Brimhall, G.H., 2007. Integration of geochemical mass balance with sediment transport to calculate rates of soil chemical weathering and transport on hillslopes. J. Geophys. Res. -Earth Surf. 112.

Yoo, K., Mudd, S.M., 2008. Toward process-based modeling of geochemical soil formation across diverse landforms: A new mathematical framework. Geoderma 146, 248-260.

Table 1. Site data and soil characteristics for studied profiles. Sites are sorted top to bottom by increasing concavity-convergence

Site ID	Curvature	Thickness (cm)		Free carbonate depth (cm)	Taxonomy	Full profile mass (g cm^{-2})			OC/ N	OC /IC	A horizon / full profile (%)		
		Full profile	A horizon			OC§	N‡	IC†			OC	N	IC
95	-0.213	38	6	6	Calcic Haploxerolls	0.58	0.08	0.4	7.4	1.4	38	31	7
18	-0.156	59	32	0	Calcic Haploxerolls	0.96	0.12	0.4	8.2	2.7	87	80	69
94	-0.091	27	27	4	Calcic Haploxerolls	0.52	0.06	0.1	8.1	6	100	100	100
91	-0.088	39	13	29	Calcic Haploxerolls	0.69	0.08	0.1	8.4	5.3	58	54	22
93	-0.051	107	10	1	Calcic Haploxerolls	0.62	0.14	1.6	4.5	0.4	40	20	4
20	-0.046	87	25	87	Calcic Haploxerolls	0.77	0.09	0.7	8.7	1.1	60	55	13
90	-0.031	83	10	24	Calcic Pachic Haploxerolls	1.16	0.14	1	8.5	1.2	30	26	6
97	-0.025	228	5	5	Calcic Pachic Haploxerolls	1.81	0.26	1.8	7.1	1	7	5	01
92	-0.007	101	18	18	Calcic Haploxerolls	0.99	0.09	0.4	11.1	2.4	50	14	2
19	-0.004	308	46	46	Calcic Pachic Haploxerolls	2.68	0.31	2.6	8.7	1	40	34	3
17	-0.004	110	23	49	Calcic Haploxerolls	1.36	0.15	0.8	8.8	1.8	41	38	0
14	0.005	387	29	29	Calcic Pachic Haploxerolls	2.36	0.29	2.8	8.2	0.8	23	18	2
96	0.014	198	15	47	Typic Haploxerepts	1.12	0.18	1.7	6.1	0.7	24	18	2
89	0.063	225	19	48	Calcic Haploxerolls	2.46	0.31	1.1	7.8	2.2	18	17	2
98	0.064	126	52	52	Calcic Pachic Haploxerolls	1.12	0.16	0.6	7	1.9	59	50	0
15	0.076	451	17	not detected	Pachic Haploxerolls	4.28	0.41	0.2	10.3	25	16	14	0

§ OC, organic carbon

‡ N, nitrogen

† IC, inorganic carbon

Table 2. Correlation coefficients between slope gradient (β), specific catchment area (As), and compound topographic index (CTI) and soil properties (n = 16).

LSP‡	Soil thickness	Depth of A horizon	Free carbonate depth	OC stock§	N stock	IC stock†	%OC	%N	%IC
β	0.293	0.116	0.241	0.086	0.124	0.556*	-0.634**	-0.697**	0.266
As	0.251	0.061	0.318	0.386	0.458	-0.009	-0.140	-0.141	-0.282
CTI	0.497	0.219	0.385	0.624**	0.677**	0.005	-0.243	-0.262	-0.445

Note: * and ** indicate significant correlations at the α= 0.01 and 0.05 levels, respectively.
‡ LSP, land surface parameter
§ OC, organic carbon
† IC, inorganic carbon

Table 3. Multiple linear regression models that predict soil thickness, stocks of soil organic carbon (OC), nitrogen (N), and inorganic C (IC), and their concentrations using forward selection. Initial input of independent variables included slope aspect (A), mean curvature (Cs), specific catchment area (As), slope gradient (β), and compound topographic index (CTI).

	Equation	R^2
Soil thickness (T, cm)	$T = 255 + 1009 * Cs - 101 * A$	0.51
Soil OC stock (g cm^{-2})	$OC = 2.2 + 7.8 * Cs - 0.84 * A$	0.50
Soil N stock (g cm^{-2})	$N = -0.029 + 0.041 * CTI$	0.42
Soil IC stock (g cm^{-2})	$IC = 0.12 + 3.1 * \beta$	0.26
Soil %OC	$\%OC = 1.6 - 1.6 * \beta – 0.087* CTI$	0.56
Soil %N	$\%N = 0.12 - 0.11 * \beta – 0.22 * Cs$	0.62
Soil %IC	NA‡	NA

‡ No model was selected.

Figure Captions

Fig. 1. The study site at the University of California's Sedgwick Reserve. White dots and numbers indicate the soil pits. Inset map indicates study location. Pits #89-#98 were located on a south-facing slope. Pits #14-#20 were on a northwest-facing slope.

Fig. 2. Effects of soil thickness on a) soil organic carbon (OC) stock, b) nitrogen (N) stock, c) inorganic C (IC) stock, d) organic C concentration (%OC), e) nitrogen concentration (%N), and f) inorganic C concentration (%IC) in full soil profiles. P values indicate the significance level of linear regressions.

Fig. 3. Correlation coefficients (r) between a) mean curvature (Cs), b) specific catchment area (As), and c) compound topographic index (CTI) and soil thickness, depth of A horizon, and free carbonate depth (n = 16). Dashed lines indicate the threshold beyond which r becomes significant at $\alpha = 0.05$ level. Grey box indicates a range of resolutions that are suitable for modeling soil C and N stocks. Arrow indicates the spatial resolution (14 m) selected for soil modeling.

Fig. 4. Relationships between curvature (Cs) and a) soil thickness, b) depth of A horizon, c) free carbonate depth, d) soil organic carbon (OC) stock, e) nitrogen (N) stock, f) inorganic C (IC) stock, g) organic C concentration (%OC), h) nitrogen concentration (%N), and i) inorganic C concentration (%IC) in full soil profiles. P values indicate the significance level of linear regressions.

Fig. 5. Effects of north-facing (N, n = 6) versus southing-facing (S, n = 10) slopes on a) soil thickness, b) depth of A horizon, c) free carbonate depth, d) soil organic carbon (OC) stock, e) nitrogen (N) stock, f) inorganic C (IC) stock, g) organic C concentration (%OC),

h) nitrogen concentration (%N), and i) inorganic C concentration (%IC) in full soil profiles. P values indicate the significance level of Student's t-tests.

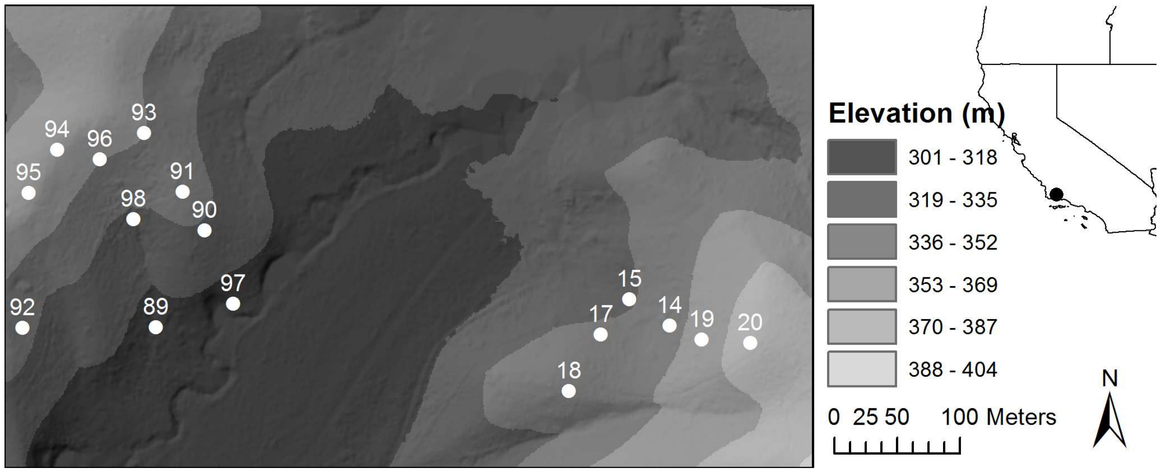
94
93
96
95
91
98
90
97
92
89
15
14
17
19
20
18
Elevation (m)
301 - 318
319 - 335
336 - 352
353 - 369
370 - 387
388 - 404
0 25 50 100 Meters
N

Fig. 1

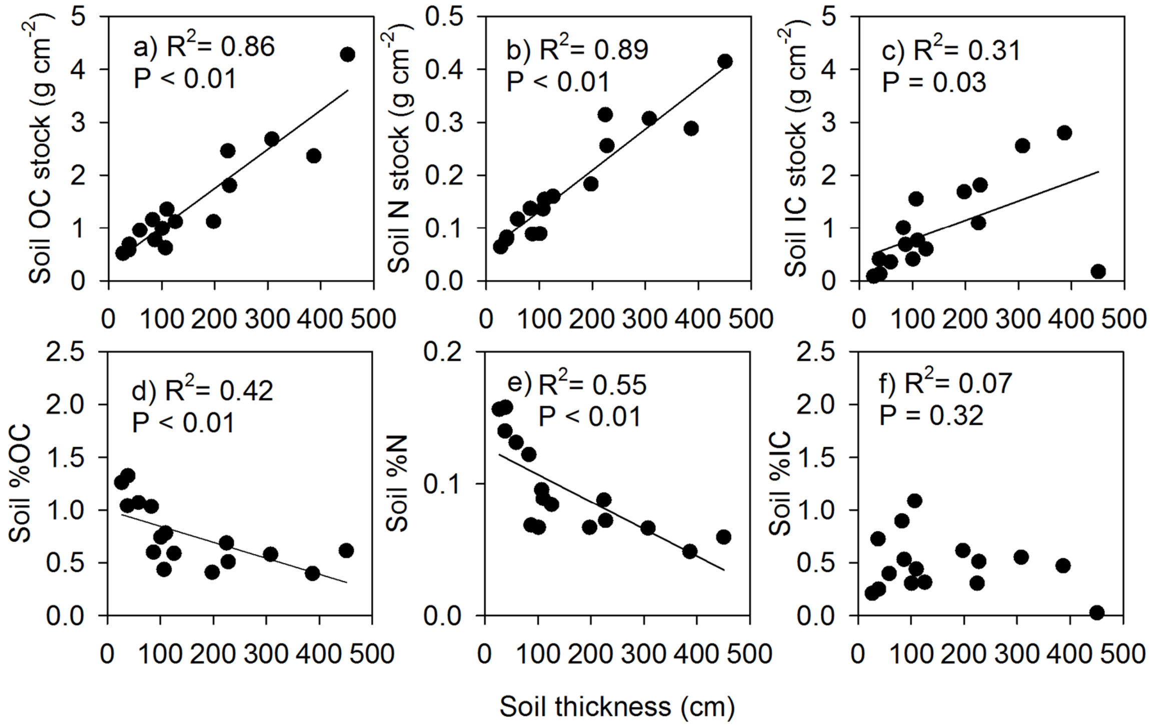

a) R2= 0.86
P < 0.01
b) R2= 0.89
P < 0.01
c) R2= 0.31
P = 0.03
d) R2= 0.42
P < 0.01
e) R2= 0.55
P < 0.01
f) R2= 0.07
P = 0.32
Soil OC stock (g cm-2)
Soil N stock (g cm-2)
Soil IC stock (g cm-2)
Soil %OC
Soil %N
Soil %IC
Soil thickness (cm)

Fig. 2

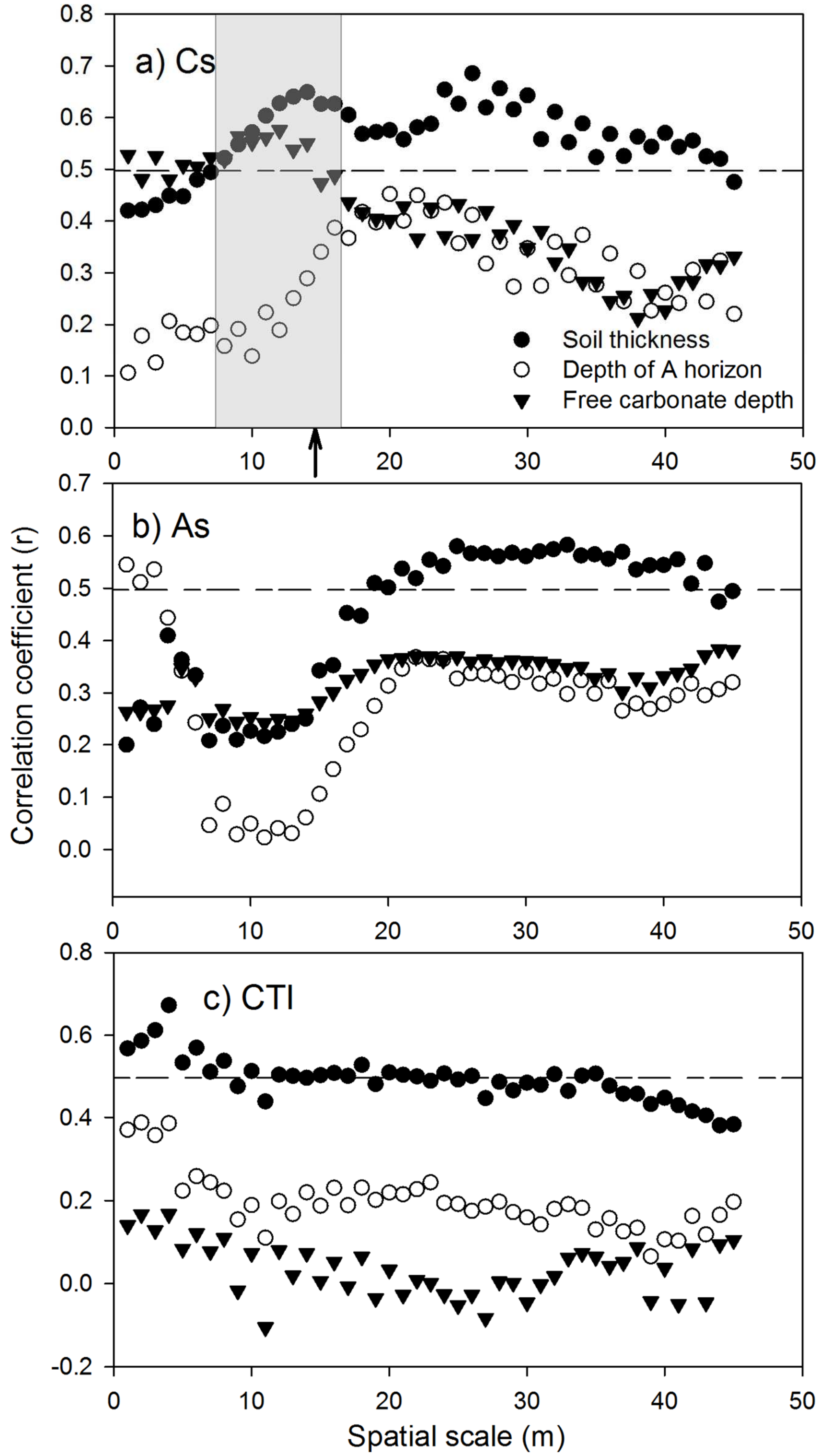
a) Cs
b) As
c) CTI
Soil thickness
Depth of A horizon
Free carbonate depth
Correlation coefficient (r)
Spatial scale (m)
0.8
0.7
0.6
0.5
0.4
0.3
0.2
0.1
0.0
-0.2
0
10
20
30
40
50

645

646 Fig. 3

647

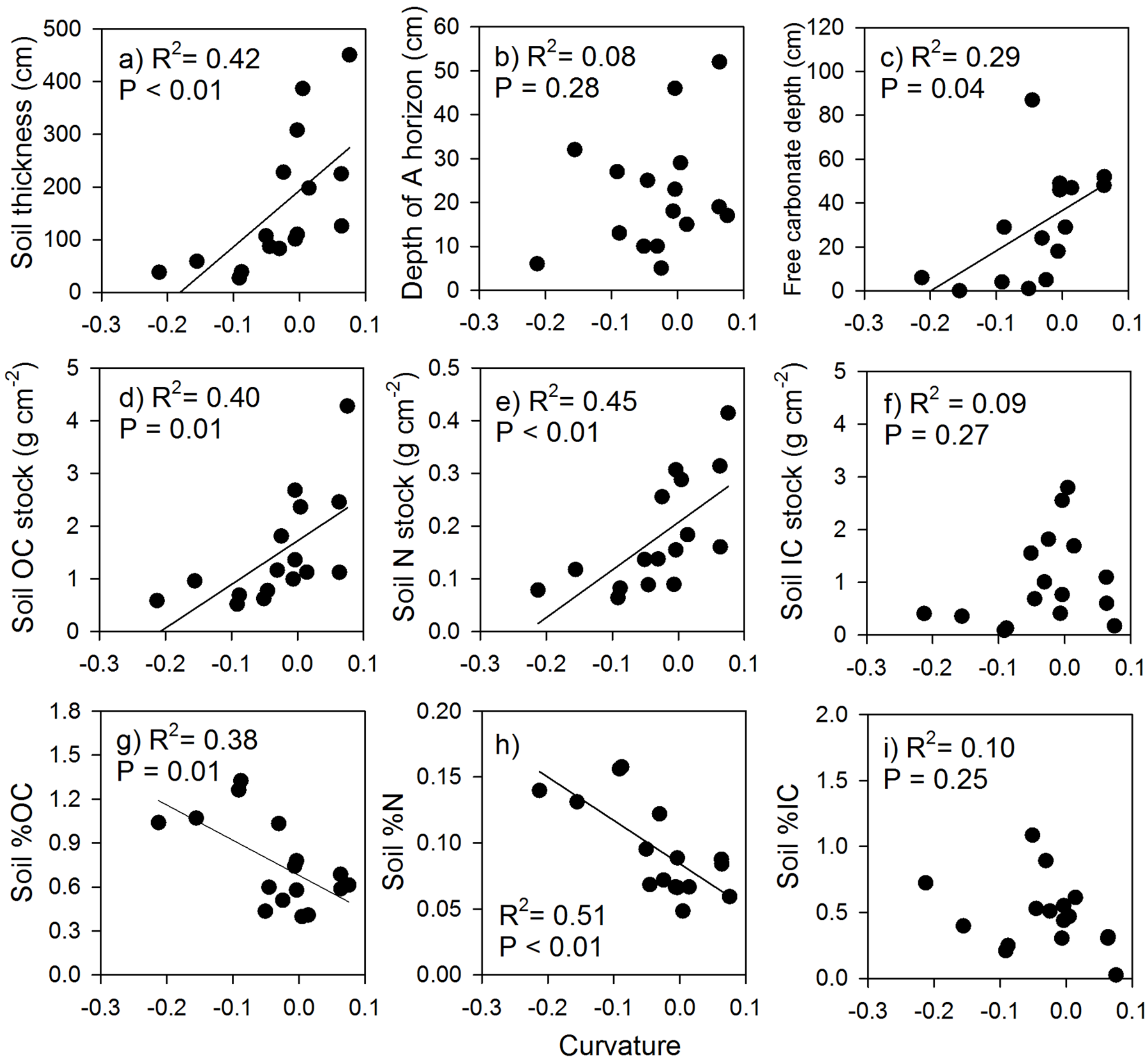

a) R^2= 0.42
P < 0.01
Soil thickness (cm)
b) R^2= 0.08
P = 0.28
Depth of A horizon (cm)
c) R^2= 0.29
P = 0.04
Free carbonate depth (cm)
d) R^2= 0.40
P = 0.01
Soil OC stock (g cm^{-2})
e) R^2= 0.45
P < 0.01
Soil N stock (g cm^{-2})
f) R^2 = 0.09
P = 0.27
Soil IC stock (g cm^{-2})
g) R^2= 0.38
P = 0.01
Soil %OC
h)
R^2= 0.51
P < 0.01
Soil %N
i) R^2= 0.10
P = 0.25
Soil %IC
Curvature

648 Fig. 4

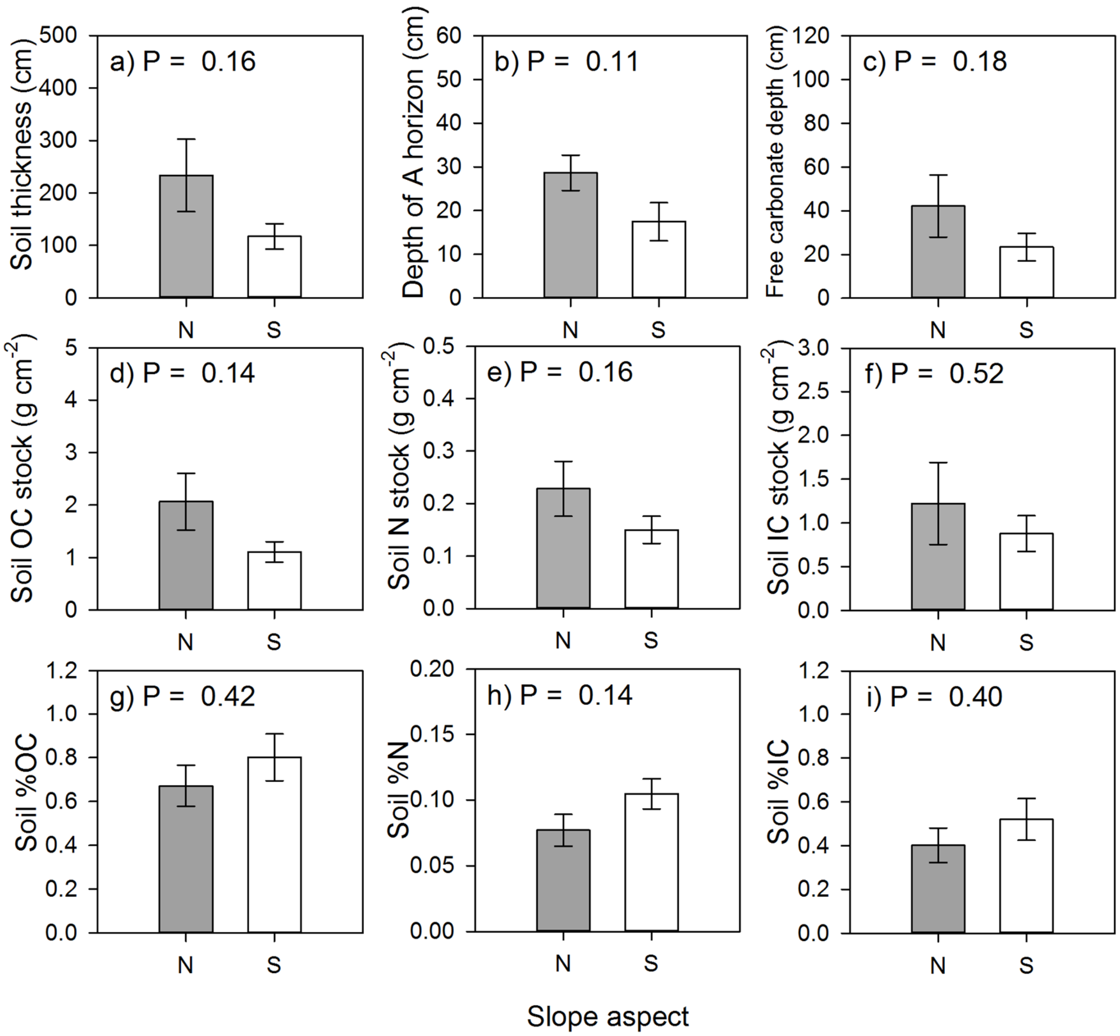
a) P = 0.16
Soil thickness (cm)
b) P = 0.11
Depth of A horizon (cm)
c) P = 0.18
Free carbonate depth (cm)
d) P = 0.14
Soil OC stock (g cm-2)
e) P = 0.16
Soil N stock (g cm-2)
f) P = 0.52
Soil IC stock (g cm-2)
g) P = 0.42
Soil %OC
h) P = 0.14
Soil %N
i) P = 0.40
Soil %IC
N
S
Slope aspect

Fig. 5

Supplementary Table 1. Soil characteristics of the studied horizons by horizons.

Pit	Hor	Lower depth	Color	Structure	Gravel	pH	Bulk density§	<2mm size fraction					
								C_{Inorg}	C_{Org}	N	C_{Inorg}	C_{Org}	N
		cm		size / type	%	(H_2O)	g cm^{-3}	----------- % ----------			-------- g cm^{-2} -------		
14	A1	6	10YR 4/1	tk pl	3.2	7.4	1.61	0.06	1.93	0.17	0.01	0.19	0.02
14	A2	29	10YR 5/1	co pr	8.1	7.9	1.50	0.17	1.01	0.10	0.06	0.35	0.04
14	Bk1	65	10YR 5/1	co pr	6.7	8.1	1.47	0.49	0.61	0.07	0.26	0.32	0.04
14	Bk1	143	10YR 5/2	co pr	7.3	8.2	1.51	0.67	0.39	0.05	0.79	0.46	0.06
14	Bk2	179	10YR 5/2		4.0	8.5	1.59	0.54	0.37	0.04	0.31	0.21	0.02
14	Bk2	215	10YR 5/2		4.7	8.6	1.58	0.50	0.38	0.04	0.28	0.22	0.02
14	Bk2	241	10YR 5/2		4.0	8.6	1.59	0.45	0.28	0.04	0.18	0.12	0.02
14	Bk2	270	10YR 5/1		3.8	8.6	1.59	0.38	0.26	0.04	0.18	0.12	0.02
14	BkC	324	2.5Y 6/2		6.4	8.7	1.55	0.40	0.23	0.03	0.34	0.19	0.03
14	BkC	360	2.5Y 6/2		8.2	8.8	1.52	0.37	0.24	0.04	0.20	0.13	0.02
14	BkC	387	2.5Y 6/2		8.6	8.8	1.51	0.47	0.14	0.03	0.19	0.06	0.01
15	A1	8	2.5Y 5/2	co gr	6.8	6.6	1.36	0.00	3.41	0.29	0.00	0.37	0.03
15	A2	17	2.5Y 5/2	co sbk	7.2	7.0	1.48	0.00	2.22	0.21	0.00	0.29	0.03
15	Bw1	38	10YR 4/1	co pr	5.0	7.0	1.55	0.00	2.03	0.19	0.00	0.66	0.06
15	Bw1	97	10YR 4/1	co pr	4.1	7.5	1.58	0.00	0.92	0.08	0.00	0.85	0.08
15	Bw2	140	10YR 4/2	co pr	2.4	8.2	1.62	0.01	0.56	0.05	0.00	0.39	0.04
15	Bw2	167	10YR 4/2		6.1	8.3	1.57	0.03	0.47	0.04	0.01	0.20	0.02
15	Bw2	212	10YR 4/2		8.1	8.4	1.54	0.03	0.36	0.04	0.02	0.25	0.03
15	Bw3	251	10YR 4/2		7.8	8.3	1.54	0.05	0.34	0.03	0.03	0.21	0.02
15	Bw3	267	10YR 4/2		6.9	8.3	1.56	0.03	0.34	0.03	0.01	0.09	0.01
15	Bw3	307	10YR 4/2		7.6	8.2	1.55	0.04	0.35	0.03	0.02	0.22	0.02
15	Bw4	331	10YR 5/2		8.7	8.2	1.53	0.04	0.30	0.03	0.01	0.11	0.01
15	Bw4	351	10YR 5/2		7.3	8.0	1.55	0.02	0.51	0.05	0.00	0.16	0.02
15	Bw4	383	10YR 5/2		4.5	8.1	1.60	0.03	0.33	0.04	0.02	0.17	0.02
15	Bw5	410			5.0	8.2	1.59	0.05	0.33	0.04	0.02	0.14	0.02
15	Bw5	451			14.6	8.1	1.43	0.02	0.28	0.04	0.01	0.16	0.02
17	A1	5	2.5Y 5/2	m sbk	5.0	6.8	1.56	0.00	2.46	0.24	0.00	0.19	0.02
17	Bw	23	2.5Y 4/1	m pr	5.0	7.1	1.54	0.00	1.32	0.14	0.00	0.36	0.04
17	Bw	49	2.5Y 4/1	co pr	5.0	7.9	1.55	0.14	0.78	0.09	0.06	0.31	0.04
17	Bk	95	2.5Y 5/1	co pr	5.0	8.1	1.61	0.68	0.54	0.06	0.50	0.40	0.05
17	BCk	110	2.5Y 5/2	ma	5.0	8.3	1.63	0.83	0.36	0.05	0.20	0.09	0.01
17	Ck1	154	2.5Y 7/2		4.4	8.5	1.62	0.76	0.09	0.02	0.54	0.07	0.02
17	Ck2	176	2.5Y 7/2		13.7	8.4	1.46	0.22	0.19	0.02	0.07	0.06	0.01
17	C	221	2.5Y 7/2		30.2	8.3	1.18	0.27	0.12	0.02	0.14	0.06	0.01
18	A1	8	2.5Y 5/2	m sbk	14.0	7.4	1.35	0.49	2.31	0.25	0.05	0.25	0.03
18	A2	32	10YR 5/1	co sbk	5.8	7.6	1.42	0.53	1.57	0.18	0.18	0.53	0.06
18	ACk	59	2.5Y 6/2	ma	0.0	7.8	1.54	0.26	0.29	0.05	0.11	0.12	0.02
18	Ck	90	2.5Y 8/1	ma	0.0	8.1	1.56	4.48	0.00	0.04	2.17	0.00	0.02
19	A1	5	10YR 5/1	co gr	5.0	7.4	1.41	0.04	2.36	0.22	0.00	0.17	0.02
19	A2	46	2.5Y 4/2	m sbk	5.0	7.8	1.50	0.11	1.58	0.15	0.07	0.97	0.09
19	Bk1	88	2.5Y 5/2	m pr	5.0	8.0	1.49	0.39	0.67	0.07	0.24	0.42	0.05
19	Bk1	155	2.5Y 5/2	co pr	5.0	8.2	1.53	0.70	0.42	0.05	0.71	0.43	0.05
19	Bk2	181	10YR 4/2	m pr	5.0	8.4	1.57	0.96	0.40	0.04	0.39	0.16	0.02
19	Bk2	192	10YR 4/2		6.4	7.9	1.53	0.42	0.86	0.09	0.07	0.14	0.02
19	Bk3	225	2.5Y 6/2		16.9	8.3	1.36	0.61	0.39	0.05	0.28	0.17	0.02
19	Bk3	291	2.5Y 6/2		6.7	8.5	1.53	0.69	0.22	0.04	0.69	0.22	0.04
19	BC	308	2.5Y 6/3		10.6	7.7	1.46	0.35	0.11	0.03	0.09	0.03	0.01
19	Ck	358	2.5Y 7/3		4.9	8.6	1.56	0.30	0.09	0.03	0.23	0.07	0.02
19	C	416	2.5Y 7/3		27.7	8.7	1.18	0.49	0.15	0.02	0.34	0.10	0.02
20	A1	7	2.5Y 5/3	m gr	10.7	7.1	1.27	0.07	2.90	0.28	0.01	0.26	0.02
20	A2	25	2.5Y 5/3	m pr	8.1	7.8	1.49	0.31	0.76	0.09	0.08	0.20	0.02
20	AC	61	2.5Y 6/3	co pr	8.2	8.0	1.54	0.50	0.30	0.05	0.28	0.17	0.03
20	AC	87	2.5Y 6/3	co pr	10.6	8.1	1.47	0.83	0.38	0.03	0.32	0.14	0.01
20	Ck	104	2.5Y 6/2	ma	15.0	8.3	1.54	0.58	0.08	0.02	0.15	0.02	0.01
89	A1	5	2.5Y 5/2	m sbk	4.0	4.5	1.19	0.18	1.69	0.19	0.01	0.10	0.01
89	A2	19	2.5Y 5/2	m sbk	3.7	7.2	1.48	0.05	1.67	0.20	0.01	0.35	0.04

89	Bw	48	2.5Y 5/2	m pr	1.1	7.1	1.58	0.01	1.27	0.15	0.00	0.58	0.07
89	Bk1	90	2.5Y 5/1	m pr	7.7	7.3	1.52	0.19	0.69	0.09	0.12	0.44	0.06
89	Bk2	115	2.5Y 5/2	vc pr	2.5	7.7	1.63	0.34	0.54	0.07	0.14	0.22	0.03
89	Bk2	135	10YR 5/1		2.8	7.7	1.66	0.36	0.68	0.06	0.12	0.23	0.02
89	Bk2	175	10YR 5/1		2.6	8.0	1.66	0.44	0.37	0.06	0.29	0.25	0.04
89	Bk3	210	10YR 6/1		2.8	8.0	1.65	0.46	0.38	0.06	0.27	0.22	0.03
89	Bk3	225	10YR 6/1		3.9	7.9	1.64	0.53	0.32	0.06	0.13	0.08	0.01
90	A	10	2.5Y 5/2	m sbk	4.0	6.9	1.40	0.42	2.50	0.25	0.06	0.35	0.04
90	Bw	24	2.5Y 5/2	co pr	2.6	7.3	1.48	0.63	1.09	0.14	0.13	0.23	0.03
90	Bk	55	2.5Y 5/2	co pr	3.1	7.3	1.31	0.84	0.92	0.11	0.34	0.37	0.05
90	Bk	83	2.5Y 5/2	m pr	2.6	7.5	1.33	1.27	0.57	0.07	0.48	0.21	0.03
90	C1	106	2.5Y 5/2	m sbk	13.1	7.5	1.17	1.36	0.31	0.05	0.37	0.08	0.01
90	C2	130	2.5Y 6/4	ma	3.9	7.8	1.87	1.08	0.10	0.03	0.48	0.05	0.02
91	A1	5	2.5Y 5/2	co pl	9.3	6.7	1.33	0.17	2.64	0.27	0.01	0.18	0.02
91	A2	13	2.5Y 5/2	m pr	9.0	7.0	1.38	0.15	2.04	0.24	0.02	0.23	0.03
91	Bw	29	2.5Y 5/2	co pr	11.2	7.4	1.35	0.21	1.06	0.14	0.05	0.23	0.03
91	Bk	39	2.5Y 6/3	m sbk	18.0	7.5	1.27	0.44	0.45	0.06	0.06	0.06	0.01
91	Ck	78	2.5Y 7/3	ma	11.5	7.6	1.57	0.41	0.17	0.03	0.25	0.10	0.02
92	A1	5	2.5Y 5/2	m sbk	16.0	6.7	1.25	0.10	2.03	0.20	0.01	0.13	0.01
92	A2	18	2.5Y 5/2	co sbk	10.7	7.1	1.44	0.00	1.96	0.00	0.00	0.37	0.00
92	Bk1	31	2.5Y 5/2	m pr	11.0	7.4	1.39	0.16	0.67	0.10	0.03	0.12	0.02
92	Bk1	53	2.5Y 5/2	m pr	13.0	7.4	1.29	0.24	0.57	0.08	0.07	0.16	0.02
92	Bk2	101	2.5Y 6/3	m pr	15.0	7.9	1.30	0.48	0.35	0.06	0.30	0.22	0.04
92	C	119		ma	19.0	8.3	1.46	0.52	0.07	0.06	0.14	0.02	0.01
93	A1	1	2.5Y 5/2	m pl	3.4	7.5	1.55	0.42	1.69	0.20	0.01	0.03	0.00
93	A2	10	2.5Y 6/3	m sbk	2.6	7.7	1.45	0.45	1.68	0.18	0.06	0.22	0.02
93	Bk	42	2.5Y 5/2	vc pr	2.6	8.0	1.46	0.84	0.66	0.11	0.39	0.31	0.05
93	Bk	65	2.5Y 5/2	m pr	4.9	8.1	1.39	1.18	0.31	0.08	0.38	0.10	0.03
93	BkC	107	2.5Y 6/2	m pr	11.6	8.2	1.18	1.45	-0.07	0.06	0.71	-0.03	0.03
93	Ck	124	2.5Y 6/3	ma	19.0	8.3	1.39	0.78	0.13	0.08	0.18	0.03	0.02
94	A	4	2.5Y 4/2	m sbk	6.6	7.5	1.32	0.15	2.73	0.28	0.01	0.14	0.01
94	Bk	27	2.5Y 4/2	co pr	4.1	7.9	1.55	0.22	1.04	0.14	0.08	0.37	0.05
94	Ck	65	2.5Y 6/2	ma	8.0	8.3	2.00	0.77	0.29	0.05	0.59	0.22	0.04
95	A	6	2.5Y 5/2	m sbk	1.0	7.5	1.38	0.33	2.68	0.30	0.03	0.22	0.02
95	Bk	20	2.5Y 5/2	m pr	2.1	8.1	1.57	0.62	0.90	0.13	0.14	0.20	0.03
95	Bk	38	2.5Y 5/2	m pr	8.5	8.1	1.43	0.94	0.63	0.10	0.24	0.16	0.03
95	C	69	2.5Y 6/2	ma	8.0	8.3	1.51	0.33	0.16	0.05	0.15	0.08	0.02
96	A	5	2.5Y 5/2	m gr	7.9	7.5	1.33	0.15	1.54	0.18	0.01	0.10	0.01
96	Bw1	15	2.5Y 5/2	m pr	2.6	7.8	1.47	0.14	1.11	0.15	0.02	0.16	0.02
96	Bw2	47	2.5Y 3/2	co pr	4.0	7.9	1.50	0.47	0.57	0.09	0.22	0.27	0.04
96	Bk1	117	2.5Y 5/2	co pr	6.1	8.1	1.39	0.70	0.34	0.06	0.68	0.34	0.06
96	Bk2	134	2.5Y 6/2	m sbk	4.5	8.1	1.47	0.73	0.22	0.05	0.18	0.05	0.01
96	Bk3	150	2.5Y 5/2		8.3	8.4	1.40	0.59	0.23	0.05	0.13	0.05	0.01
96	Bk3	166	2.5Y 5/2		8.0	8.4	1.40	0.66	0.26	0.05	0.15	0.06	0.01
96	BCk	198	2.5Y 6/2		19.9	8.6	1.22	0.74	0.22	0.04	0.29	0.09	0.02
97	A	5	2.5Y 5/2	m abk	4.4	7.7	1.38	0.18	1.69	0.19	0.01	0.12	0.01
97	Bk1	35	2.5Y 5/2	co pr	2.3	7.6	1.56	0.41	0.91	0.12	0.19	0.43	0.06
97	Bk2	79	2.5Y 5/1	vc pr	2.8	7.8	1.59	0.60	0.60	0.09	0.42	0.42	0.06
97	Bk2	116	2.5Y 6/1	vc pr	2.0	8.0	1.67	0.68	0.32	0.06	0.42	0.20	0.04
97	Bk3	181	2.5Y 5/1		7.5	8.0	1.55	0.48	0.39	0.06	0.49	0.39	0.06
97	Bk3	201	2.5Y 5/2		9.6	8.1	1.51	0.38	0.21	0.04	0.12	0.06	0.01
97	Bk4	210	2.5Y 5/2		4.0	8.4	1.56	0.00	0.84	0.00	0.00	0.12	0.00
97	Bk4	219	2.5Y 5/2		4.8	8.6	1.53	0.59	0.37	0.05	0.08	0.05	0.01
97	BC	228	2.5Y 6/2		9.1	8.6	1.31	0.75	0.22	0.05	0.09	0.03	0.01
98	A1	7	2.5Y 5/1	m abk	6.9	6.6	1.49	0.00	0.84	0.05	0.00	0.09	0.01
98	A2	21	2.5Y 5/1	co pr	3.2	7.3	1.55	0.00	1.10	0.14	0.00	0.24	0.03
98	A2	52	2.5Y 5/2	co pr	3.1	7.6	1.54	0.00	0.70	0.09	0.00	0.33	0.04
98	Bk	126	2.5Y 6/1	co pr	2.8	8.1	1.50	0.54	0.41	0.07	0.60	0.46	0.08

§ <2mm fraction, COLE-adjusted based on estimated 33% clay content

Supplementary Figures

Supplementary Fig. 1 Relationships between curvature and soil organic C stock (OC, g cm^{-2}), nitrogen stock (N, g cm^{-2}), inorganic C stock (IC, g cm^{-2}), organic C concentration (%OC), nitrogen concentration (%N), and inorganic C concentration (%IC). Figure is horizontally divided into two panels. Upper panel shows the data from A horizon, and lower panel shows the data from subsoil.

Supplementary Fig. 2 Predicted spatial distributions of a) soil thickness, b) soil organic C (OC) stock, and c) organic C concentration (%OC) using models in Table 3. Black dots and numbers indicate sampling locations as in Fig. 1.

Supplementary Fig. 3 Relationships between soil thickness and curvature (Cs) at a) 1-m, b) 14-m, and c) 31-m resolutions; 14-m resolution was used in soil modeling.

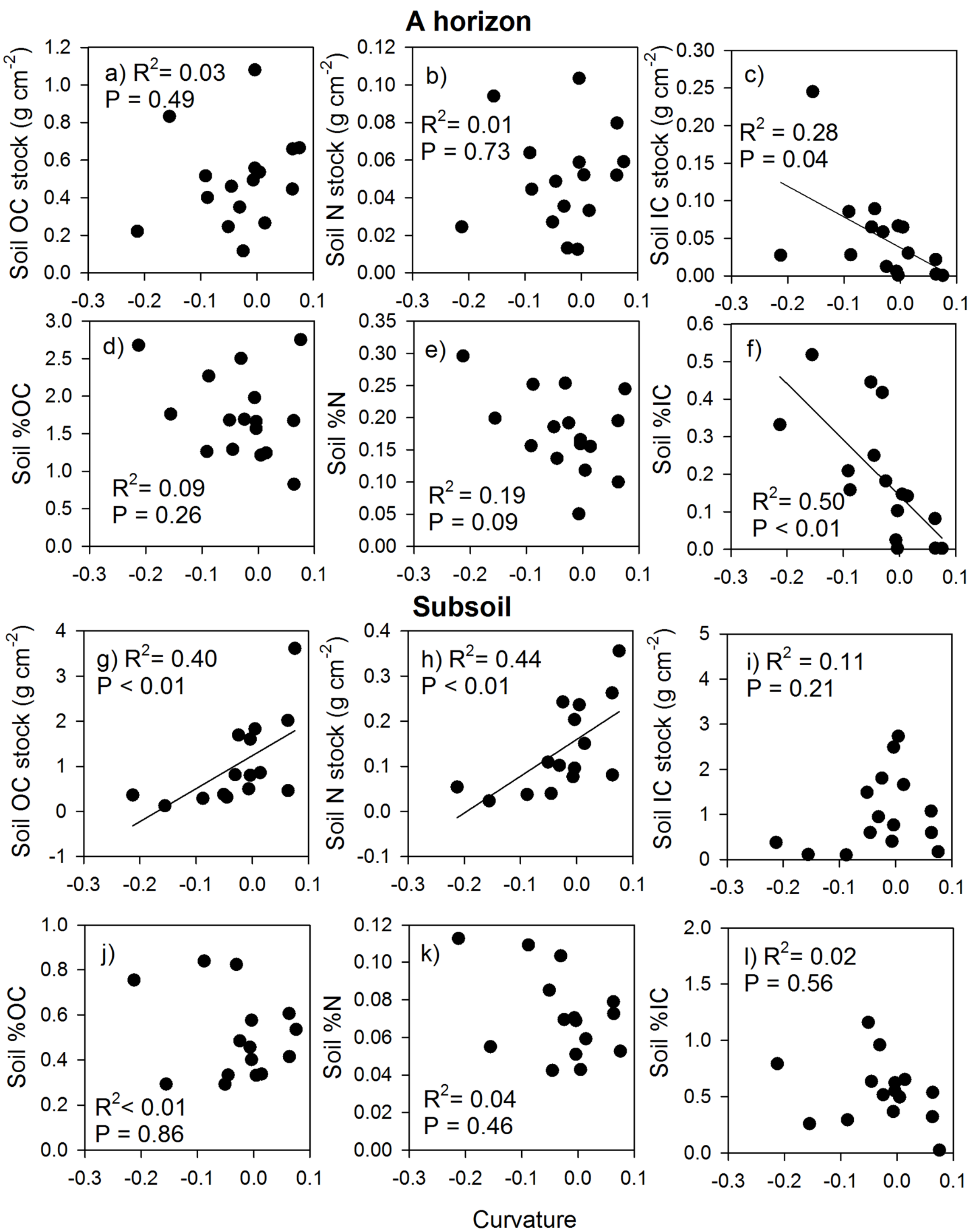

Supplementary Fig. 1

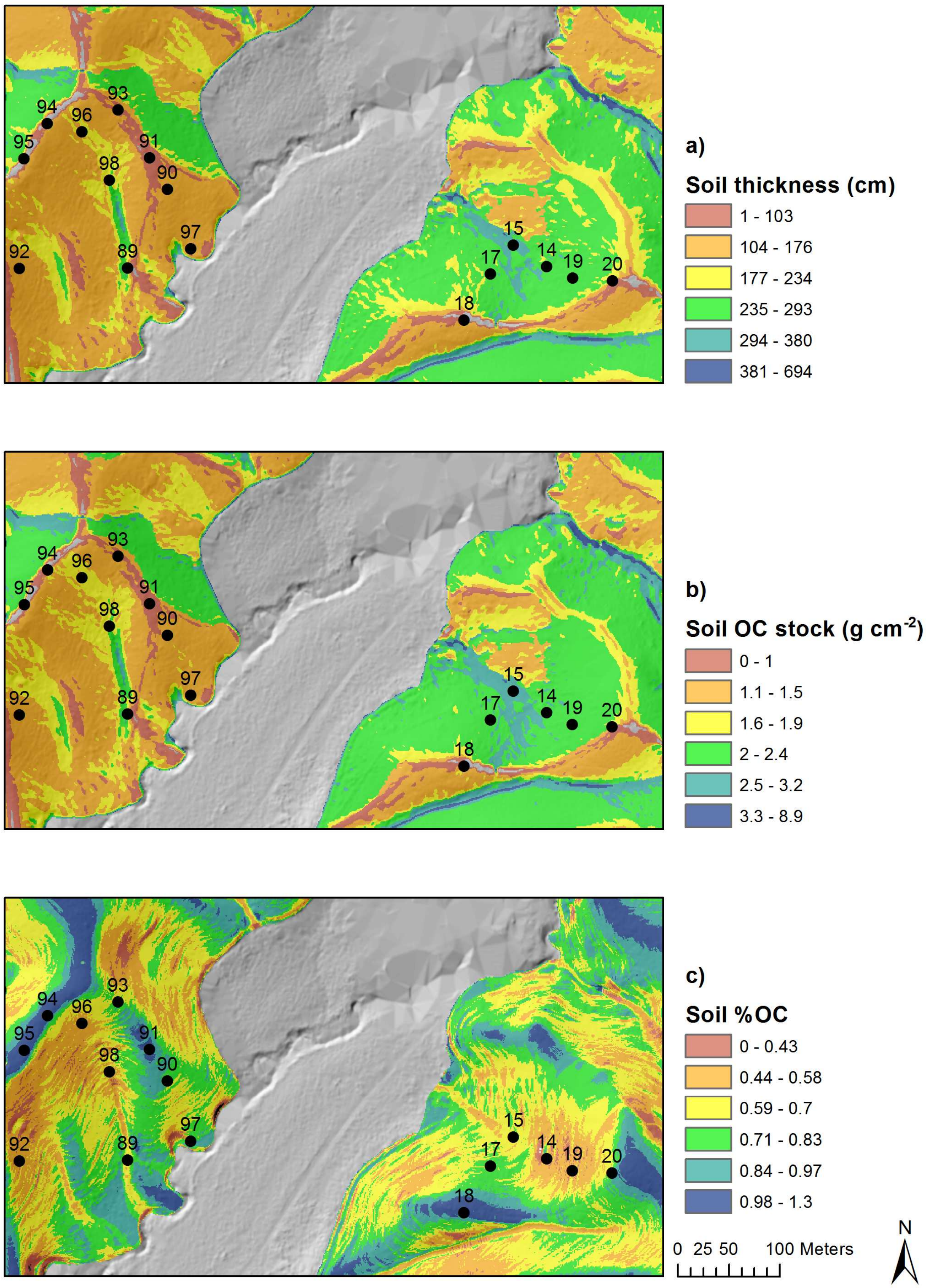

Supplementary Fig. 2

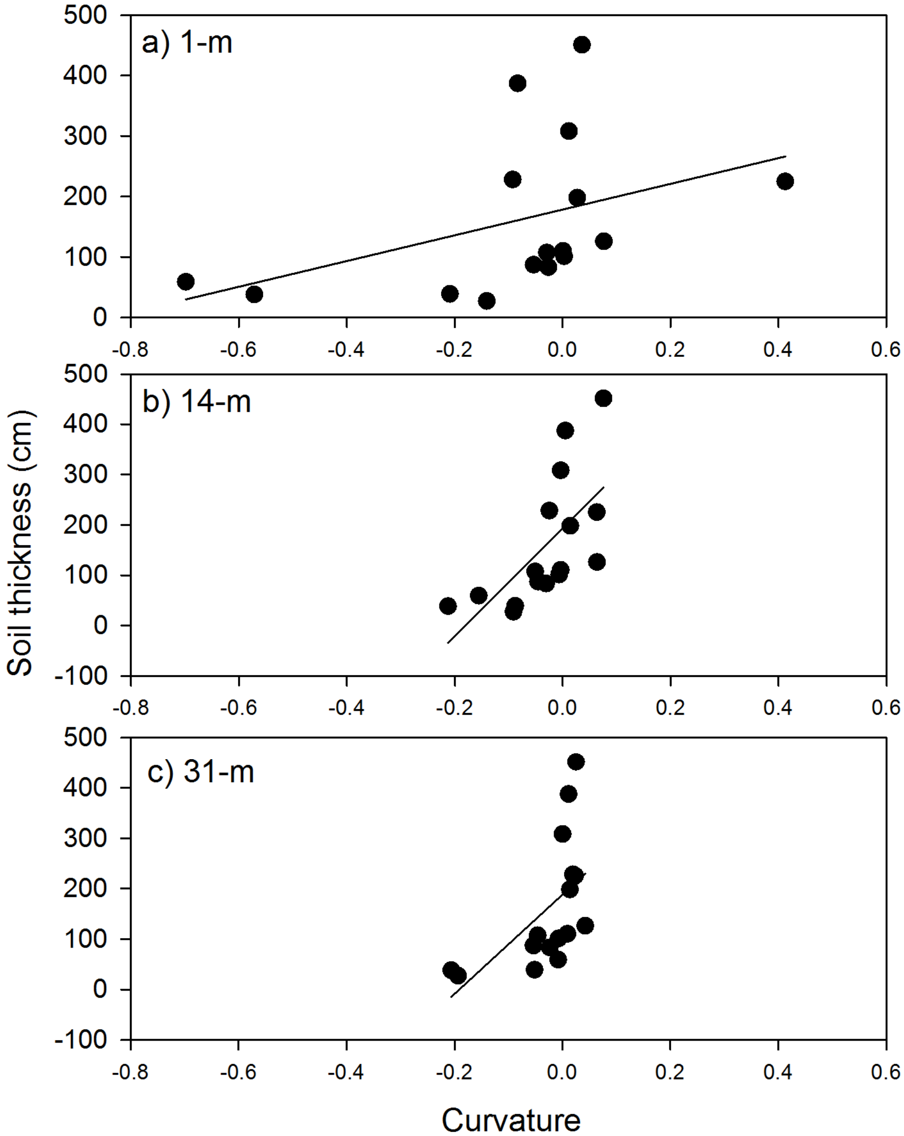

22

23 Supplementary Fig. 3